La_2O_3对 MGH956 合金 TIG 焊焊缝组织和性能的影响

雷玉成，　赵　凯，　黄　巍，　梁申勇
（江苏大学 材料科学与工程学院，镇江　212013）

摘　要：为了研究 La_2O_3 对焊缝组织和性能的影响，分别以未填加、填加 2% 和 4% La_2O_3 的填充材料对 MGH956 合金进行 TIG 焊接，应用光学显微镜、扫描电镜和透射电镜对焊缝的微观组织和拉伸断口进行观察，同时测试焊缝的抗拉强度. 结果表明，适当提高 La_2O_3 含量，可以使焊缝晶粒得到细化，填加 2% La_2O_3 的焊缝晶粒最细小均匀，焊缝中的颗粒相增多且分布均匀，强化机制是由细晶强化和 Orowan 强化共同作用，但当 La_2O_3 加入量达到 4% 时，发现颗粒相有团聚现象，强化主要由位错塞积引起. 填加 2% La_2O_3 的焊缝抗拉强度最大，为 628 MPa，拉伸断口为韧—脆混合断裂.

关键词：MGH956 合金；TIG 焊；组织；力学性能
中图分类号：TG444　　**文献标识码**：A　　**文章编号**：0253－360X(2013)10－0001－04

雷玉成

0　序　　言

MGH956 合金是采用机械合金化方法制造的氧化物弥散强化(oxide dispersion strengthened，ODS)高温合金，合金中均匀分布着高热稳定性和化学稳定性的纳米 Y_2O_3 颗粒对基体进行强化[1]，性能优异[2]. 目前国外学者对 ODS 合金的摩擦焊和搅拌摩擦焊研究较多[3－5]，然而电弧焊具有适用性强，操作简单等优势，因此研究 ODS 合金电弧焊对推广 ODS 合金的应用有一定意义.

稀土元素中以 La 元素的性质最为活泼，而且 La 元素的脱硫率最高[6]，适量稀土 La 元素对焊缝能起到净化和变质作用，但填加纯 La 元素极易氧化，因此通过填加含有不同 La_2O_3 的填充材料对 MGH956 合金进行 TIG 焊，以期通过 La_2O_3 达到细化晶粒，提高接头性能的目的.

1　试验方法

试验材料选用 1.3 mm 厚的 MGH956 合金，合金的化学成分如表 1 所示. 试验使用 MW3000 逆变全数字化钨极氩弧焊机进行焊接，焊接电流 72 A，电弧电压 12 V，焊接速度 1.8 mm/s，钨极直径为 2.4 mm，采用直流正接，纯度为 99.9% 的氩气作为保护气体，气体流量为 8 L/min，三种填充材料的具体化学成分如表 2 所示.

表 1　MGH956 合金化学成分(质量分数，%)
Table 1　Chemical compositions of MGH956 alloy

Cr	Al	Ti	Y_2O_3	O	N	C	Fe
19.64	5.06	0.52	0.4	0.22	0.02	0.007	余量

表 2　三种填充材料的化学成分(质量分数，%)
Table 2　Chemical compositions of three filler materials

Ni	Cr	Mn	Si	C	Ti	Al	La_2O_3	Fe
32	21	1	0.35	0.3	1.2	1.35	—	余量
32	21	1	0.35	0.3	1.2	1.35	2	余量
32	21	1	0.35	0.3	1.2	1.35	4	余量

试板尺寸为 70 mm×35 mm×1.3 mm，焊后沿焊缝横向制取金相试样，用光学显微镜对焊缝微观组织进行观察，腐蚀液为 10% HNO_3 + 10% HF + 80% H_2O(质量分数). 用扫描电子显微镜对拉伸断口和焊缝颗粒形貌进行观察，采用透射电子显微镜对焊缝组织微结构进行观察，拉伸试验在 Instron 电子万能试验机上进行，拉伸速度为 1 mm/min.

2　试验结果与讨论

2.1　焊接接头组织及拉伸性能

图 1 为焊缝的微观组织形貌，可以看出，未填加

收稿日期：2012－08－09
基金项目：国家自然基金资助项目(51075191)；江苏省高校博士创新基金资助项目(CXZZ11_0556)；江苏大学科技创新团队资助项目(JD0805)；江苏高校优势学科建设工程资助项目

La_2O_3 焊缝晶粒粗大，并且分布有较多气孔，填加 La_2O_3 后，焊缝晶粒明显细化，气孔数量明显减少，而且填加 2% La_2O_3 的焊缝晶粒最细小均匀. 这是由于 La_2O_3 在电弧的高温下发生分解，即熔池中会过渡部分 La 原子，La 原子半径很大(0.187 nm)，且是表面活性元素，在焊缝凝固过程中会在液—固界面前沿富集，减小成分过冷，增大过冷度和形核率，从而使晶粒细化. 焊缝中镧极易与硫、氧等发生化学反应生成 La_2O_2S，La_2O_3 等化合物[7]，这些化合物一部分聚集成渣，净化了焊缝，一些高熔点的化合物在焊缝凝固过程中可以成为异质形核核心，研究表明[8]，初生 γ 相的最密排面(111)在 La_2O_3 的(0001)面上形核的点阵错配度为 8%(错配度大于 12% 认为核心无效)，这说明 La_2O_3 成为非均质形核核心是有效的. 同时 La_2O_3 会增加合金的熔化潜热，减小液—固凝固区间，降低了熔池中合金元素的扩散和运动，进一步阻碍晶粒长大. 适量的 La_2O_3 还能够降低 Ni-Cr-Al 等合金体系熔点[9]，提高熔池流动性，从而使生成气体容易逸出，进一步减少焊缝中气孔. 当加入过多的 La_2O_3 时，潜在的形核质点可能团聚，导致真正能够成为形核质点的数量减少，从而导致焊缝晶粒粗化且大小不均匀，如图 1c 所示.

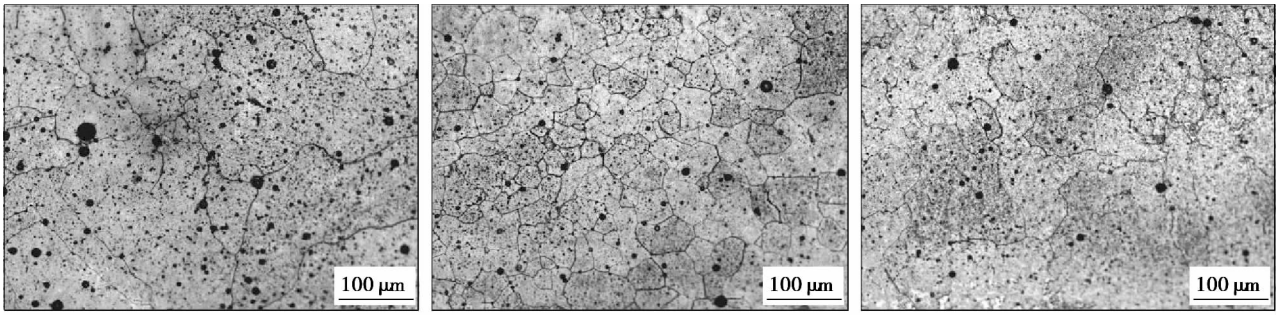

(a) 未添加 La_2O_3 (b) 2% La_2O_3 (c) 4% La_2O_3

图 1 填加不同 La_2O_3 焊缝中心的微观组织

Fig. 1 Weld microstructure with different La_2O_3

图 2 为焊缝的 SEM 形貌，未填加 La_2O_3 时，焊缝中生成的颗粒相较少，而且发现有规则几何形状的颗粒，能谱分析表明颗粒主要为 TiC 和 TiN(图 3a). 填加 2% La_2O_3 时，焊缝中颗粒相明显增多，分布更加均匀，规则几何形状的颗粒变成了圆形或近球形. 能谱分析表明，焊缝中除了含有 TiN 等颗粒外，还含有 Al_2O_3(图 3b)等颗粒，但当 La_2O_3 的添加量达到 4% 时，颗粒相发生了严重的团聚现象.

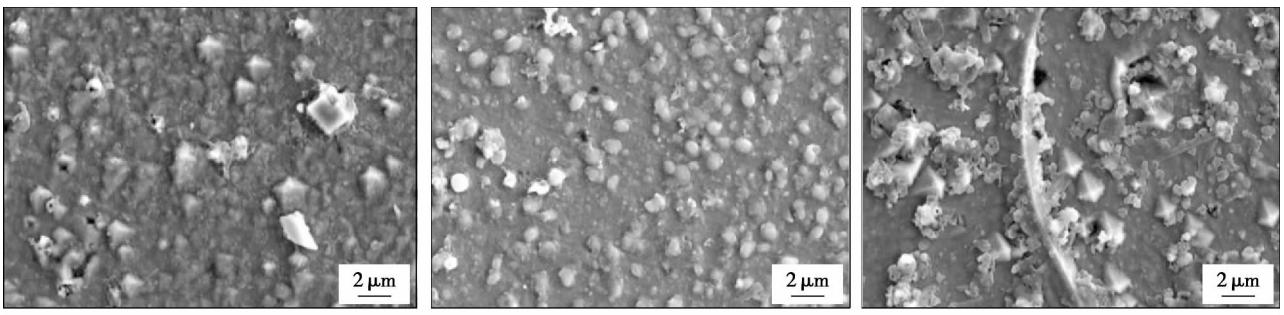

(a) 未添加La_2O_3 (b) 2%La_2O_3 (c) 4%La_2O_3

图 2 填加不同 La_2O_3 焊缝的 SEM 形貌

Fig. 2 SEM photograph of joints with different La_2O_3

由此可以看出，适量的 La_2O_3 能够促进颗粒相的弥散分布，对焊缝起到弥散强化作用，这是由于 La_2O_3 进入焊缝中会与熔池中的其它元素(如 O 元素等)生成稳定的微小化合物，这些化合物一方面净化了焊缝，另一方面可以起到变质核心的作用，使颗粒相的形核核心增多，聚集长大的机会减少，更多的颗粒相只能在原生位置结晶长大，从而使颗粒相更多的生成并且弥散分布，同时 La_2O_3 的存在也使

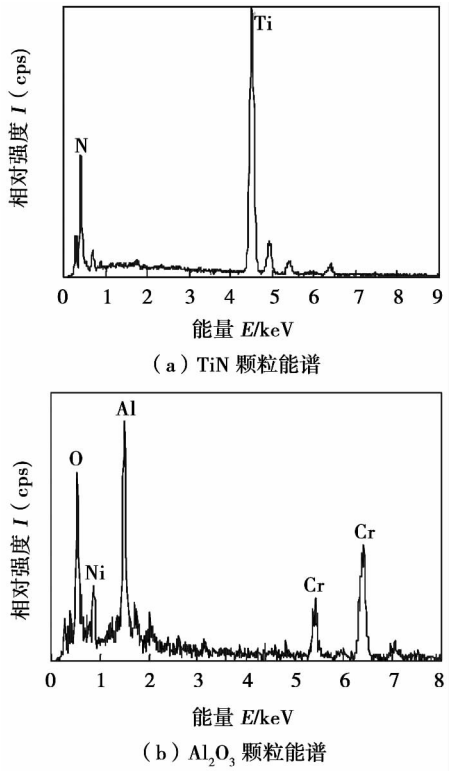

图 3　焊缝中颗粒能谱

Fig. 3　EDS analysis of particles in joints

焊缝晶粒细化，微观晶界增加，进一步阻碍合金原子的扩散和运动，使颗粒相不容易聚集长大，分散更加均匀. 研究表明[10]，焊缝中的 La_2O_3 不仅可以细化焊缝晶粒，生成的微小化合物还可以成为 TiC 等颗粒的形核核心，增加了 TiC 弥散分布的几率. 但当 La_2O_3 的添加量达到 4% 时，熔池单位体积内异质核心增多，生成的颗粒相彼此之间距离变小，所以容易发生团聚现象.

试验根据国家标准 GB/T228—2002《金属材料室温拉伸试验方法》制取拉伸试样，取三个试样平均值作为拉伸试验结果，如表 3 所示.

表 3　试样抗拉强度(R_m/MPa)

Table 3　Tensile strength of samples

未填加 La_2O_3	2% La_2O_3	4% La_2O_3
553	628	587

由表 3 可以看出随着 La_2O_3 含量的增加，焊缝的抗拉强度先升高后降低，填加 2% La_2O_3 的焊缝抗拉强度最高，为 628 MPa，这是因为填加 2% La_2O_3 后气孔数量明显减少，焊缝有效截面积增加，焊缝中颗粒相弥散分布，有助于提高焊缝强度. 同时焊缝晶粒得到细化，晶粒细化后，增加了阻碍裂纹扩展的晶界的面积，有助于减轻晶界上杂质元素的偏聚浓度而避免沿晶脆性断裂. 当焊缝中加入 4% La_2O_3 时，焊缝强度有所下降，这是因为与未填加 La_2O_3 的焊缝相比，焊缝晶粒有所细化，气孔有所减少，但没有填加 2% La_2O_3 焊缝晶粒细小均匀；另外焊缝中的颗粒相发生了团聚，粗大颗粒相数量增多，在外加应变场中，颗粒相发生损伤的速度随着尺寸的增大而加快[11]，因此颗粒增强相的团聚和粗化会使其在较低的外应力作用下发生断裂，而且颗粒相的团聚也会导致焊缝中局部颗粒相的体积分数提高，使内应力增加，进而促使颗粒相断裂.

图 4a 为未填加 La_2O_3 的焊缝的拉伸断口，断口呈明显河流状花样，总体表现出脆性穿晶解理断裂，而填加 La_2O_3 的焊缝断口河流花样特征不明显，而且出现大片韧窝，说明焊缝存在一些韧性，从断口形貌可判定断裂特征为韧性脆性混合断裂，如图 4b 和图 4c 所示.

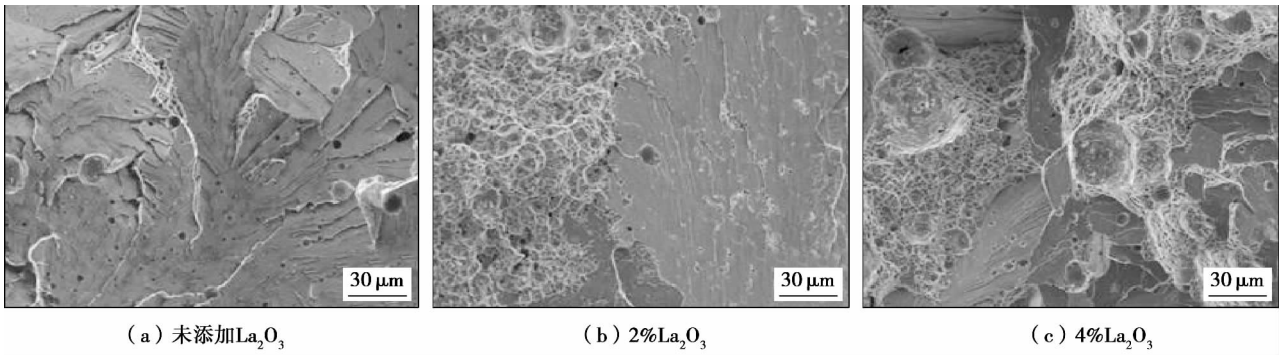

图 4　填加不同 La_2O_3 焊缝的断口 SEM 形貌

Fig. 4　SEM fractographs of joints with different La_2O_3

2.2　接头微观强化机理分析

图 5a 是未填加 La_2O_3 时焊缝的 TEM 形貌，可以看出焊缝中位错密度较低，颗粒相很少，而填加 2% La_2O_3 的焊缝中均匀分布着纳米级的增强颗粒

和大量的位错,当位错运动时,邻近的其它位错会对其产生阻碍作用,产生位错强化. 根据第二相颗粒与滑移位错的交互作用机制并结合图 5b 可以看出,位错是通过 Orowan 机制绕过增强颗粒的,图 5b 中 A 处为位错绕过颗粒相的初始阶段,可以看出位错线已经开始弯曲,B 处为位错绕过颗粒相的过程,C 处为位错绕过颗粒相后留下的位错环. 当滑移位错以 Orowan 机制绕过不可变形颗粒时,位错发生弯曲会增大位错的线张力,此时若使位错绕过颗粒相继续滑移就需要更大的外加应力,因此导致焊缝强化.

当颗粒相尺寸较小时,位错是以 Orowan 机制绕过颗粒相的,但当位错遇到尺寸较大的颗粒相或者晶界、亚晶界等阻碍时,位错将会在阻碍物前不断沉积形成位错塞积,此时微观结构细化和位错塞积起到主要的强化作用[11]. 图 5c 是填加 4% La_2O_3 焊缝的 TEM 形貌,可以看出焊缝中颗粒相分布不均匀,存在颗粒相团聚现象,在颗粒团聚处形成位错塞积(图 5c 中箭头处),而远离塞积处位错密度很低,因此结合以上分析及图 2c 和图 5c,可以认为填加 4% La_2O_3 的焊缝位错塞积起到主要强化作用.

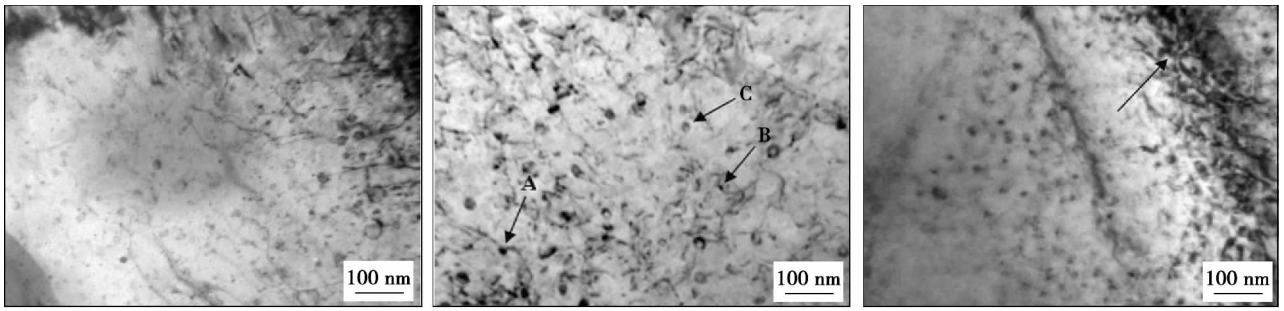

(a) 未添加La_2O_3 (b) 2%La_2O_3 (c) 4%La_2O_3

图 5 填加不同 La_2O_3 焊缝的 TEM 形貌

Fig. 5 TEM photograph of joints with different La_2O_3

3 结 论

(1) 焊缝中加入 La_2O_3 后组织得到一定程度的细化,当加入 2% La_2O_3 时焊缝组织最细小均匀,颗粒相生成较多,且弥散分布,提高了焊缝的强度,但当 La_2O_3 填加量达到 4% 时,发现颗粒相有团聚现象.

(2) 随着 La_2O_3 含量的增加,焊缝强度先升高后降低,拉伸断口由脆性解理断裂变为韧 - 脆混合断裂. 填加 2% La_2O_3 焊缝的强化是由于晶粒细化和 Orowan 强化共同作用,而填加 4% La_2O_3 焊缝的强化主要由位错塞积引起.

参考文献:

[1] 淮军锋, 郭万林, 李天文, 等. 氧化物弥散强化高温合金 MGH956 的基本焊接性研究[J]. 材料工程, 2008(9): 52 - 55.
Huai Junfeng, Guo Wanlin, Li Tianwen, *et al*. Weldabilities of the oxide-dispersion-strengthened superalloy MGH956 [J]. Chinese Journal of Materials Engineering, 2008(9): 52 - 55.

[2] 张 胜, 侯金保, 郭德伦, 等. MGH956 合金 TLP 连接机理及接头组织分析[J]. 焊接学报, 2004, 25(3): 43 - 47.
Zhang Sheng, Hou Jinbao, Guo Delun, *et al*. Transient liquid phase bonding mechanism and mi crostrueture of MGH956 joints [J]. Transactions of the China Welding Institution, 2004, 25(3): 43 - 47.

[3] Chen C L, Tatlock G J, Jones A R . Microstructural evolution in friction stir welding of nanostructured ODS alloys [J]. Journal of Alloys and Compounds, 2010, 504: 460 - 466.

[4] Uwaba T, Ukai S, Nakai T. Properties of friction welds between 9Cr-ODS martensitic and ferritic-martensitic steels [J]. Journal of Nuclear Materials, 2007, 367/370: 1213 - 1217.

[5] Noh S, Kasada R, Kimura A, *et al*. Microstructure and mechanical properties of friction stir processed ODS ferritic steels [J]. Journal of Nuclear Materials, 2011, 417: 245 - 248.

[6] 杜 挺. 稀土碱土等元素的物理化学及在材料中的应用[M]. 北京: 科学出版社, 1995.

[7] 张小城, 张卫平. 焊缝内夹杂物的热力学分析[J]. 焊接学报, 1994, 15(3): 172 - 178.
Zhang Xiaocheng, Zhang Weiping. Thermodynamic analysis of inclusion in weld [J]. Transactions of the China Welding Institution, 1994, 15(3): 172 - 178.

[8] 杨庆祥, 高聿为, 廖 波, 等. 夹杂物在中高碳钢堆焊金属中成为初生奥氏体非均质形核核心的探讨[J]. 中国稀土学报, 2000, 18(2): 138 - 141.
Yang Qingxiang, Gao Yuwei, Liao Bo, *et al*. Discussion of inclusions as heterogeneous nuclei of primary austenite of medium-high carbon steel during hardfacing [J]. Journal of the Chinese Rare Earths Society, 2000, 18(2): 138 - 141.

[下转第 21 页]

性能最差,从而使高频电阻焊接头在 CO_2/H_2S 腐蚀环境中产生了沟槽腐蚀.

(2) 试验钢焊缝处的大角晶界比例高于母材和热影响区,这使得焊缝区反应速度常数高于母材和热影响区,因此焊缝的腐蚀速率最高.

(3) 通过电化学分析表明,焊缝处的电极反应的极化阻力最小,腐蚀反应易于发生;而母材的电极反应的极化电阻最大,腐蚀反应不易进行. 因此在腐蚀过程中,焊缝区的腐蚀速率高于母材和热影响区,这与腐蚀试验所得结果及极化曲线分析结果一致.

参考文献:

[1] 张　雷, 丁睿明, 杨建炜, 等. 高含 H_2S/CO_2 介质中 X60 钢腐蚀产物膜分析[J]. 北京科技大学学报, 2009, 31(5): 563 -567.
Zhang Lei, Ding Ruiming, Yang Jianwei, *et al*. Analysis of corrosion scales on X60 steel under high H_2S/CO_2 content environments[J]. Journal of University of Science and Technology Beijing, 2009, 31(5): 563 -567.

[2] 丁晓丽, 斯松华, 丁志龙. 热处理对 N80 级 ERW 套管钢组织与性能的影响[J]. 热加工工艺, 2011, 40(10): 194 -196.
Ding Xiaoli, Si Songhua, Ding Zhilong. Effects of heat treatment on microstructure and properties of ERW N80 oil casings steel[J]. Material & Heat Treatment, 2011, 40(10): 194 -196

[3] 毕宗岳, 刘道新, 李　轩, 等. 热处理对 ERW 焊缝沟槽腐蚀敏感行为的影响[J]. 材料热处理学报, 2011, 32(2): 48 -54.
Bi Zongyue, Liu Daoxin, Li Xuan, *et al*. Effect of heat treatment on grooving corrosion behavior of electric resistance welded seam [J]. Transactions of Materials and Heat Treatment, 2011, 32(2): 48 -54.

[4] 史耀武, 康志新, 程建秀. 接合面氧化物夹杂对高频电阻焊管韧性的影响[J]. 焊接学报, 1993, 14(4): 207 -214.
Shi Yaowu, Kang Zhixin, Cheng Jianxiu. Effect of oxide inclusions in joint interfaces of high-frequency electrical resistance welded pipes [J]. Transactions of the China Welding Institution, 1993, 14(4): 207 -214.

[5] Bi Zongyue, Wang Rong, Jing Xiaotian. Grooving corrosion of oil coiled tubes manufactured by electrical resistance welding [J]. Corrosion Science, 2012, 57(3): 67 -73.

[6] Yoon-Seok Choi, Srdjan Nesic, Shiun Ling. Effect of H_2S on the CO_2 corrosion of carbon steel in acidic solutions [J]. Electrochimica Acta, 2011, 56: 1752 -1760.

[7] 陶勇寅, 杜则裕, 李云涛, 等. H_2S 浓度对国产 X70 管线钢及其焊接接头应力腐蚀性能的影响[J]. 焊接学报, 2004, 25(3): 105 -108.
Tao Yongyan, Du Zeyu, Li Yuntao, *et al*. Effect of H_2S on sulfide stress cracking of base metals and weldedjoints of domestic X70 pipeline steels [J]. Transactions of the China Welding Institution, 2004, 25(3): 105 -108.

[8] Ren Chengqiang, Liu Daoxin, Bai Zhenquan. Corrosion behavior of oil tube steel in simulant solution with hydrogen sulfide and carbon dioxide [J]. Materials Chemistry and Physics, 2005, 93(2/3): 305 -309.

[9] 徐连勇, 荆洪阳, 曹　军, 等. 管线钢焊接接头 H2S 应力腐蚀试验分析[J]. 焊接学报, 2010, 31(1): 12 -16.
Xu Lianyong, Jing Hongyang, Cao Jun, *et al*. H_2S stress corrosion invertigation of pipeline steel welded [J]. Transactions of the China Welding Institution, 2010, 31(1): 12 -16.

作者简介: 武会宾,男,1977 年出生,博士,副教授. 主要从事高强耐腐蚀钢的研发工作. 发表论文 80 余篇. Email: wuhb@ustb.edu.cn

[上接第 4 页]

[9] 王丽芳, 满达虎. 镧含量对衬板用高锰钢组织和性能的影响[J]. 材料热处理技术, 2009, 38(16): 22 -28.
Wang Lifang, Man Dahu. Effect of lanthanum content on structure and properties of high manganese steel for lining board [J]. Material & Heat Treatment, 2009, 38(16): 22 -28.

[10] 宋思利. 钨极氨弧原位合成 TiC 增强铁基熔敷层的研究[D]. 山东: 山东大学, 2007.

[11] 张　毅, 周延春. Ti_3SiC_2 弥散氧化 Cu:一种新的弥散强化铜合金[J]. 金属学报, 2000, 36(6): 662 -666.
Zhang Yi, Zhou Yanchun. Ti_3SiC_2 dispersion-strengthened copper: a new dispersion-strengthened copper alloy [J]. Acta Metallurgica Sinica, 2000, 36(6): 662 -666.

作者简介: 雷玉成,男, 1962 年出生,教授,博士研究生导师. 主要从事焊接工艺及设备、焊接过程控制及模拟、先进材料连接技术等方面的研究与开发. 发表论文 80 余篇. Email: yclei@ujs.edu.cn

MAIN TOPICS, ABSTRACTS & KEY WORDS

Effect of La_2O_3 on microstructure and mechanical properties of MGH956 alloy during TIG welding LEI Yucheng, ZHAO Kai, HUANG Wei, LIANG Shenyong (School of Material Science and Engineering, Jiangsu University, Zhenjiang 212013, China). pp 1 – 4, 21

Abstract: In order to study the effect of La_2O_3 on joint microstructure and mechanical properties, tungsten insert gas (TIG) welding of MGH956 alloy was performed without La_2O_3 and with 2%, 4% La_2O_3 as filler materials respectively. The joint microstructure and fracture surfaces were analyzed by testing method such as optical microscope(OM), scanning electron microscope(SEM) and transmission electron microscopy(TEM). Tensile strengths were also tested. The results show that grain refinement occurs in joint when the content of La_2O_3 increases properly. When the joint contains 2% La_2O_3, joint grain is the smallest and uniformly distributed, particle-phase increases and it is uniform distributed in the joint. The strengthening mechanism of joint are fine-grain strengthening and Orowan strengthening. When the content of La_2O_3 is 4%, particles partially agglomerate in joint. The joint is strengthened mainly by piling up of dislocations. When the joint contains 2% La_2O_3, tensile strength is the largest and reaches 628 MPa. The fracture surface of joint exhibites brittle-ductile mixed fracture.

Key words: MGH956 alloy; TIG welding; microstructure; mechanical properties

Research on controlling method of size and distribution of oxide inclusions in weld metal with auxiliary electric field LI Xiaoquan, CHU Yajie, YANG Zonghui (School of Material Engineering, Nanjing Institute of Technology, Nanjing 211167, China). pp 5 – 8

Abstract: For controlling size and distribution of oxide inclusions in weld metal, a method was presented in which an auxiliary electric field was applied between molten slag and weld pool metal with submerged arc welding so as to lead ion flow in molten by making use of auxiliary electric field. The preliminary experimental research was carried out with voltage supplied by direct current power supply as auxiliary electric field. The results show that when tungsten is used as cathode of auxiliary electric field, the electric conductivity of molten slag can be greatly improved due to lots of free electrons running into molten slag, and this makes a steady directional ion flow effectively inside the molten. By making complex particles ionization inside the molten, the auxiliary electric field applied between molten slag and weld pool metal impels both positive and negative ions to produce inverse flowers and results in electrochemical reactions at interface, thus reducing the opportunity of oxidation and this is helpful for inclusions to be broken and homogeneous. Meanwhile, under auxiliary electric field, the free oxygen ion in weld pool will migrate to slag-metal interface and be preferably combined with oxide forming elements in molten slag, then enter into slag. Therefore the oxygen content in weld metal can be effectively reduced.

Key words: auxiliary electric field; molten slag; weld pool; inclusion

Experiments and numerical simulation on spot-welded structure of ultra-high strength steel YU Huiping, WANG Weiwei, LI Xiaoyang, LIU Yuehua (College of Mechanical Engineering and Applied Electronics Technology, Beijing University of Technology, Beijing 100124, China). pp 9 – 12

Abstract: Mechanical parameters of spot-welded structure of 22MnB5 ultra-high strength steel were obtained by a series of experiments including tensile-shear testing, optical experiment and the vickers-hardness testing. In addition, intensity simulations on the spot-welded structure were carried out by software ANSYS. The good agreement of simulation results with experimental data confirmed the rationality of the three-phrase finite element model of the spot-welded structure, which consist of weld nugget, plastic ring and base metal. Based on the simulation results, the plastic ring edge of the spot-welded structure interface is the weakest position, where the structural failure is mainly caused by the shear stress. For purpose of spot-welded structure optimization, the dependence of strength of the spot-welded structures on their structure parameters were analyzed. The simulations results uncovered that the maximum Von Mises stress of the structure can be reduced to a considerable extent by increasing radius of the weld nugget, the overlapping length of the two sheets and the thickness of the plates.

Key words: ultra-high strength steel; spot weld; tensile-shear experiment; numerical simulation

Seam tracking control for mobile welding robots based on dynamic model LÜ Xueqin[1], ZHANG Ke[2], WU Yixiong[2] (1. School of Automation Engineering, Shanghai University of Electric Power, Shanghai 200090, China; 2. School of Material Science and Engineering, Shanghai Jiaotong University, Shanghai 200030, China). pp 13 – 16

Abstract: As the requirement of high accuracy in seam tracking, the systems dynamics become more prominent in seam tracking process. The non-complete dynamic model for the four wheeled mobile welding robot was established. Variable structure controller with sliding mode has been designed to complete coordinately controlling of cross-slider and mobile welding robot. Several factors have been considered including the influence of the inertia, electrical machinery dynamics, surface irregularity and other factors in seam tracking process on the tracking accuracy. Through the theoretical analysis and simulation, it has been proved that the dynamic model and the variable structure controller with sliding mode are correct and valid in seam tracking. It has set up important foundation for off-line programming, simulation and dynamic control of mobile welding robot.